BULLETIN OF THE EARTHQUAKE
RESEARCH INSTITUTE
Vol. 45 (1967), pp. 945-961

48. *Soft Core Spectrum Splitting and Related Problems of the Spheroidal Oscillations of an Elastic Sphere with a Homogeneous Mantle and Core.*

By Tatsuo USAMI, Yoshiko KOTAKE and Yasuo SATÔ,

Earthquake Research Institute.

(Read Sept. 12, 1967.—Received Sept. 30, 1967.)

1. Introduction

The rigidity of the core has long been the key problem of seismology in relation to the travel time of core waves, the amplitude of core reflected waves such as *ScS* and the physical structure of the earth's interior. Recently it was made clear in various papers[1] that the core is neither perfect liquid nor rigid. The study of the core-reflected shear waves *sScS* and *ScS* has revealed that the possible maximum value of the core rigidity is 2×10^{10} c.g.s.[2] Since the average value of the rigidity of the mantle is approximately 3×10^{12} c.g. s., the ratio of the above two quantities turns out to be 1/150. This circumstance inevitably calls for the study of the effect of finite rigidity of the core on the oscillations of the earth, on the propagation of seismic waves and on the amplitude of waves reflected from and diffracted by the core.

One of these effects, the phenomenon called "Soft Core Spectrum Splitting", was found by one of the present authors[3] for the torsional oscillation of an elastic sphere with a homogeneous mantle and core. The possibility of determining the rigidity of the core using the frequencies of the torsional oscillation of the earth was examined there. When the core was a soft solid, many spectral lines appeared and the radial distribution of azimuthal amplitude in the core became large com-

1) H. JEFFREYS, *The Earth*, Cambridge, § 7.051, (1959).
F. PRESS, "Rigidity of the Earth's Core," *Science*, **124** (1956), 1204.
A. SCHLANGER, "Free Non-Rigid Vibration of the Earth," *Geofisica Pura e Applicata*, **43** (1959), 23-35.

2) D.L. ANDERSON, "Attenuation in the Mantle and Rigidity of the Core from Multiply Reflected Core Phases," *Proc. Nat. Acad. Sci.*, **51** (1964), 168-172.

3) Y. SATÔ, "Soft Core Spectrum Splitting of the Torsional Oscillation of an Elastic Sphere and Related Problems," *Bull. Earthq. Res. Inst.*, **42** (1964), 1-10.

pared to that in the mantle.

For the spheroidal oscillation, a similar phenomenon will take place. However, as the core rigidity tends to zero, it will be revealed in the present paper that the frequency of one of the radial higher modes approaches to the corresponding value for a perfect liquid core model. The amplitude distribution of these modes in the mantle tends also to that of the liquid core, but not necessarily in the part of the core.

In the present paper, the soft core spectrum splitting and the transition of physical properties of various modes from a soft solid to a perfect liquid core will be studied for the spheroidal oscillation of an elastic sphere consisting of a homogeneous mantle and a homogeneous core. The following subjects are discussed and explained: 1) the general pattern of frequency change as a function of colatitudinal order number n when the core rigidity is small, 2) the modes to be observed and the corresponding spectral amplitudes, 3) the frequency as a function of the core rigidity and the relation to the spectral amplitudes and displacement distributions, and 4) the characteristic rigidity of the core which makes the $S2(SV)$ wave in the core vanish.

2. Frequency Equation

Following the usual way of solving the wave equations referred to the polar coordinates (r, θ, φ), solutions for the spheroidal oscillation are given by

$$\begin{aligned} u &= U_n(r) \cdot P_n^m(\cos\theta) \cdot \begin{matrix}\cos\\ \sin\end{matrix} m\varphi \cdot \exp(jpt), \\ v &= V_n(r) \cdot \frac{d}{d\theta} P_n^m(\cos\theta) \cdot \begin{matrix}\cos\\ \sin\end{matrix} m\varphi \cdot \exp(jpt), \\ w &= -m V_n(r) \cdot \frac{P_n^m(\cos\theta)}{\sin\theta} \cdot \begin{matrix}\sin\\ -\cos\end{matrix} m\varphi \cdot \exp(jpt), \end{aligned} \tag{2.1}$$

where u, v and w are the radial, colatitudinal and azimuthal components of displacement respectively. U_n and V_n are the functions giving the radial distribution of displacements, and can be expressed as a sum of contributions from both P and $S2$ waves:

$$\begin{aligned} U_n(r) &= {}_P U_n(r) + {}_S U_n(r), \\ V_n(r) &= {}_P V_n(r) + {}_S V_n(r), \end{aligned} \tag{2.2}$$

where the prefixes refer to the P and $S2$ waves respectively. The functions ${}_PU_n$, ${}_PV_n$, ${}_SU_n$ and ${}_SV_n$ are expressed by the spherical Bessel functions $j_n(x)$ and $n_n(x)$. The boundary conditions, which determine frequency of the free spheroidal oscillations of an elastic sphere consisting of a homogeneous mantle and core, are

a) the vanishing of radial and colatitudinal stress components on the surface $r=a$,

b) the continuity of stress and displacement components at the core boundary $r=b$.

The frequency equation can be written in the from

$$\Delta=\begin{vmatrix} \widehat{rr}(PJ)_a & \widehat{rr}(SJ)_a & \widehat{rr}(PN)_a & \widehat{rr}(SN)_a & 0 & 0 \\ \widehat{r\theta}(PJ)_a & \widehat{r\theta}(SJ)_a & \widehat{r\theta}(PN)_a & \widehat{r\theta}(SN)_a & 0 & 0 \\ \widehat{rr}(PJ)_b & \widehat{rr}(SJ)_b & \widehat{rr}(PN)_b & \widehat{rr}(SN)_b & \widehat{rr}(P_iJ)_b & \widehat{rr}(S_iJ)_b \\ \widehat{r\theta}(PJ)_b & \widehat{r\theta}(SJ)_b & \widehat{r\theta}(PN)_b & \widehat{r\theta}(SN)_b & \widehat{r\theta}(P_iJ)_b & \widehat{r\theta}(S_iJ)_b \\ u(PJ)_b & u(SJ)_b & u(PN)_b & u(SN)_b & u(P_iJ)_b & u(S_iJ)_b \\ v(PJ)_b & v(SJ)_b & v(PN)_b & v(SN)_b & v(P_iJ)_b & v(S_iJ)_b \end{vmatrix}=0. \quad (2.3)$$

Each element of the determinant is the contribution to the stress or displacement components ($\widehat{rr}$, $\widehat{r\theta}$, u and v) from P(or $S2$) waves having j_n(or n_n) as the function ${}_PU_n, \ldots, {}_SV_n$. Suffixes a and b refer to the radius where each quantity is evaluated and i is referred to quantities in the core. When the core boundary is fixed, equation (2.3) is reduced to

$$\Delta=\bar{\Delta}(5, 6; 3, 4)\cdot R_n \quad (2.4)$$

It reducese to

$$\Delta=\bar{\Delta}(5, 6; 5, 6)\cdot L_n, \quad (2.5)$$

when the stress components on the core-mantle boundary vanish.

$$R_n=\widehat{rr}(P_iJ)_b\cdot\widehat{r\theta}(S_iJ)_b-\widehat{rr}(S_iJ)_b\cdot\widehat{r\theta}(P_iJ)_b$$

$$L_n=u(P_iJ)_b\cdot v(S_iJ)_b-u(S_iJ)\cdot v(P_iJ)_b \quad (2.6)$$

and $\bar{\Delta}(\alpha, \beta; \gamma, \delta)$ is a minor determinant obtained by eliminating columns α, β and rows γ, δ from the determinant Δ. The vanishing of $\bar{\Delta}(5, 6; 5, 6)$ is the frequency equation of the mantle's free spheroidal oscillation and $\bar{\Delta}(5, 6; 3, 4)=0$ is that of the mantle's oscillation when the inner surface

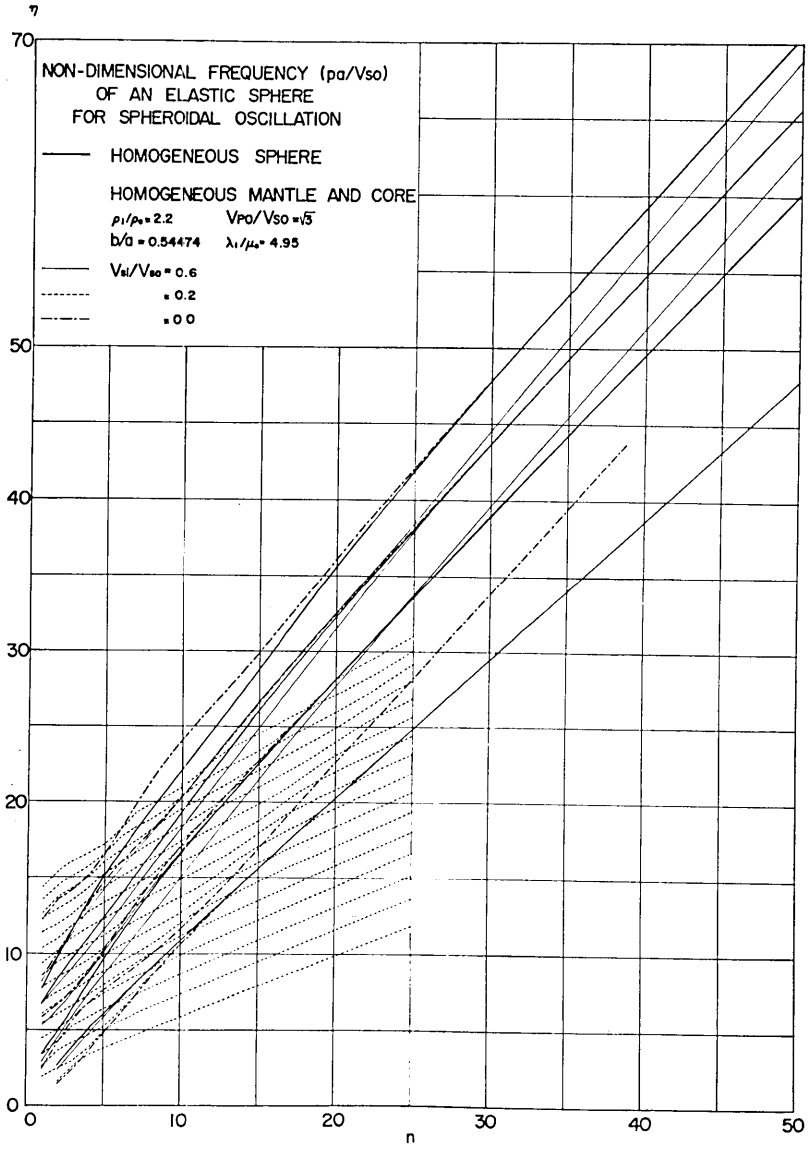

Fig. 1-a

Fig. 1. Non-dimensional frequency $\eta(=pa/V_{s0})$ of the spheroidal oscillation of an elastic sphere as a function of the colatitudinal order number n. A thick solid line shows the case for a homogeneous sphere. The other lines represent the case of a homogeneous mantle with a homogeneous core. A dotted line shows a transition phenomenon from one radial mode to the next higher one. A part of a dotted line connecting these transition segments lies along a chain line, namely, the curve for homogeneous mantle with a liquid core, and tends to a thick solid line as n increases. The thin solid line and the chain line approach to the thick solid line as n becomes large. In order to show detailed features more clearly, a part of the figure is drawn in magnified scale in Figure 1-b.

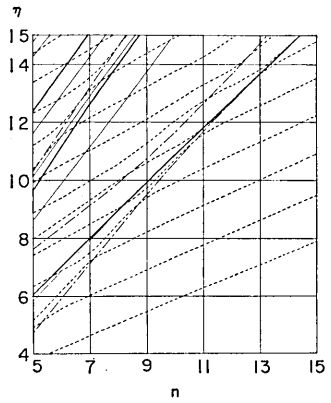

Fig. 1-b

is fixed. $L_n=0$ is the characteristic equation of the spheroidal oscillation of the core under the assumption that the surface is fixed, while $R_n=0$ is that of the free spheroidal oscillation of the core. Normalizing the function giving radial distribution of displacement so that the radial surface displacement will take value 1, the spectral amplitudes of the radial and colatitudinal components at the surface for each mode are, as was explained in a former paper[4], proportional to

$$S_n^u \propto 1/(\partial \Delta/\partial p), \quad S_n^v \propto (v/u)_{r=a}/(\partial \Delta/\partial p), \qquad (2.7)$$

where p is the frequency. These values must be evaluated at $p={}_ip_n$, the eigenfrequency of each mode.

3. Earth Model

We adopted a simple earth model, which approaches to the one used in our previous work[5] on the theoretical seismograms as the core rigidity tends to zero. The parameters characterizing this model are

b/a	$=0.544741$
a (radius of the sphere)	$=6370$ km
b (radius of the core)	$=3470$ km
ρ_i/ρ_o	$=2.2$
λ_i/μ_o	$=4.95$
$\lambda_o=\mu_o$	

where suffixes i and o refer to the quantities in the core and mantle respectively. Throughout this work the Lame's constant λ_i of the core is kept constant and the effect of gravity is neglected.

4) Y. SATÔ, T. USAMI, M. LANDISMAN and M. EWING, "Basic Study on the Oscillation of a Sphere, Part V: Propagation of Torsional Disturbance on a Radially Heterogeneous Sphere. Case of a Homogeneous Mantle with a Liquid Core," *Geophys. J.*, **8** (1963), 44-63.

5) Y. SATÔ and T. USAMI, "Propagation of Spheroidal Disturbances on an Elastic Sphere with a Homogeneous Mantle and a Core," *Bull. Earthq. Res. Inst.*, **42** (1964), 407-425.

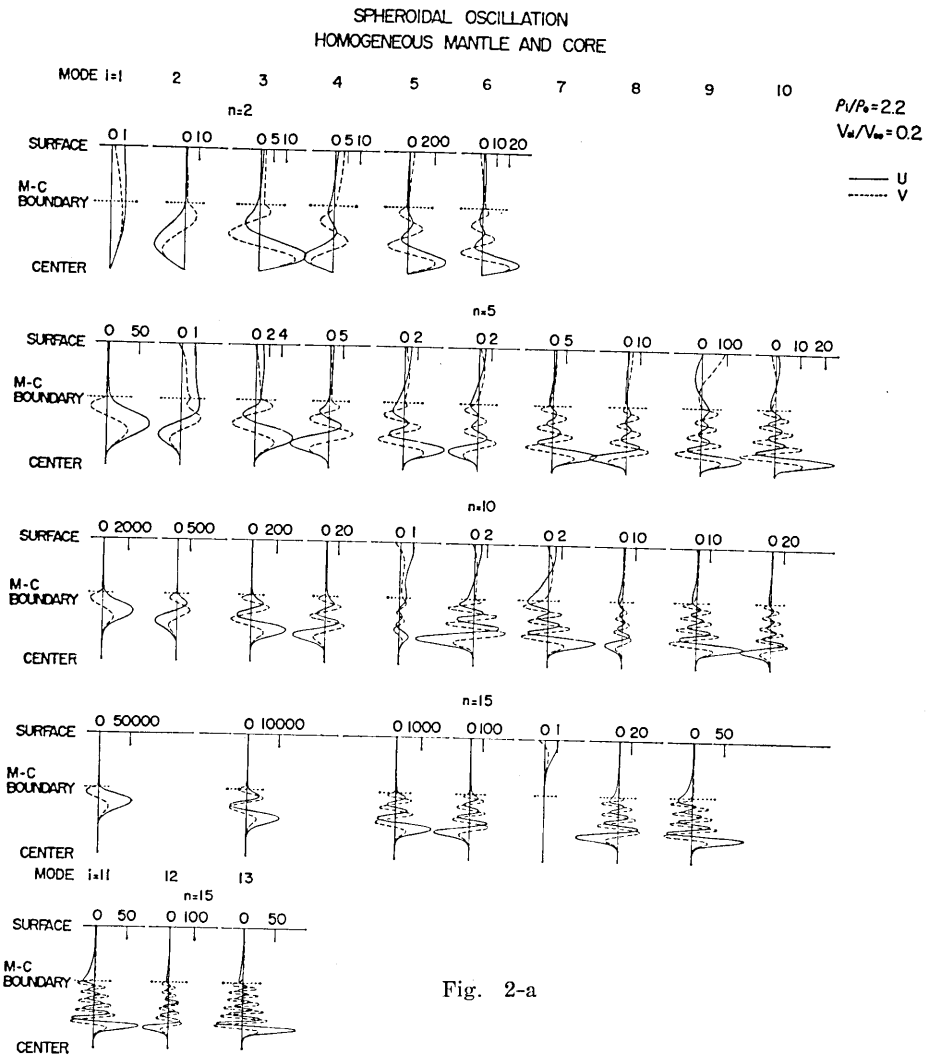

Fig. 2-a

Fig. 2. Radial distribution of displacement for the cases $\xi(=V_{Si}/V_{So})=0.2$ and 0.6. The radial amplitude on the surface is taken to be one. The solid line refers to the radial component and dotted line to the colatitudinal one.

4. Frequency as Function of Colatitudinal Order Number n and Radial Distribution of Displacement

The frequency equation (2.3) was solved for the cases $\xi(=V_{Si}/V_{So})=$ 0.2 and 0.6. $\xi=0.2$ gives an example of the case of soft core. The

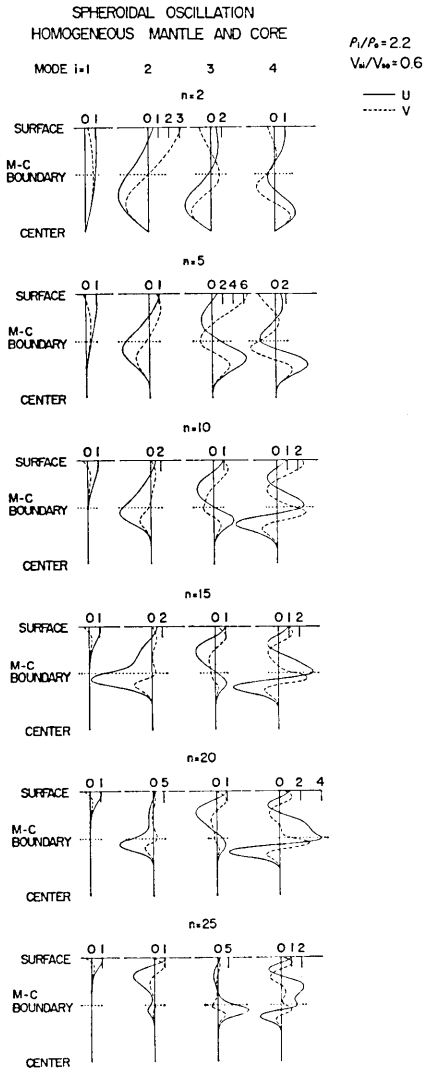

Fig. 2-b

calculated non-dimensional frequencies $\eta(=pa/V_{s_0})$ are arranged in Figure 1 together with those for the perfect fluid core and for the homogeneous sphere.

As the colatitudinal order number n increases, the frequency η for the cases $\xi=0.0$ (liquid core) and 0.6 approaches to those for a homogeneous sphere except for those on the transition segments from one radial mode to the next higher branch. The modes on these segments show large displacements near the core boundary, which is a characteristic associated with the Stoneley wave along a boundary between two different media. For the case of small core rigidity, such as $\xi=0.2$, many radial higher branches appear. They display the minor transition phenomena from one radial mode to the next higher one. The minor transition segments lie close to the curve for the liquid core and the difference between them becomes negligible as the order number n increases.

In order to see the character of various modes for the cases $\xi=0.2$ and 0.6, the radial distributions of displacements were computed and they are given in Figures 2-a and 2-b. In these figures, the radial displacement on the surface was taken to be one. For the case $\xi=0.6$, the pattern of displacement distribution of a mode resembles that of the liquid core[5], when these modes have similar values of non-dimensional frequency. For the case $\xi=0.2$ (an example of soft core), however,the displacement distributions of modes on the minor transition segments

show similar features to those of the corresponding modes for the liquid core ($\xi=0$).

The argument of the functions j_n and n_n for $S2$ waves in the core at the boundary $r=b$ is;

$$k_i b = pb/V_{Si} = \eta \cdot (b/a) \cdot (V_{So}/V_{Si}) = (\eta/\xi) \cdot (b/a).$$

When the core is soft, namely the value of ξ is small, $k_i b$ becomes large and consequently, from the asymptotic property of the spherical Bessel functions, it is easily understood that the contribution of the $S2$ wave is the cause of the large amplitude and oscillatory feature of the

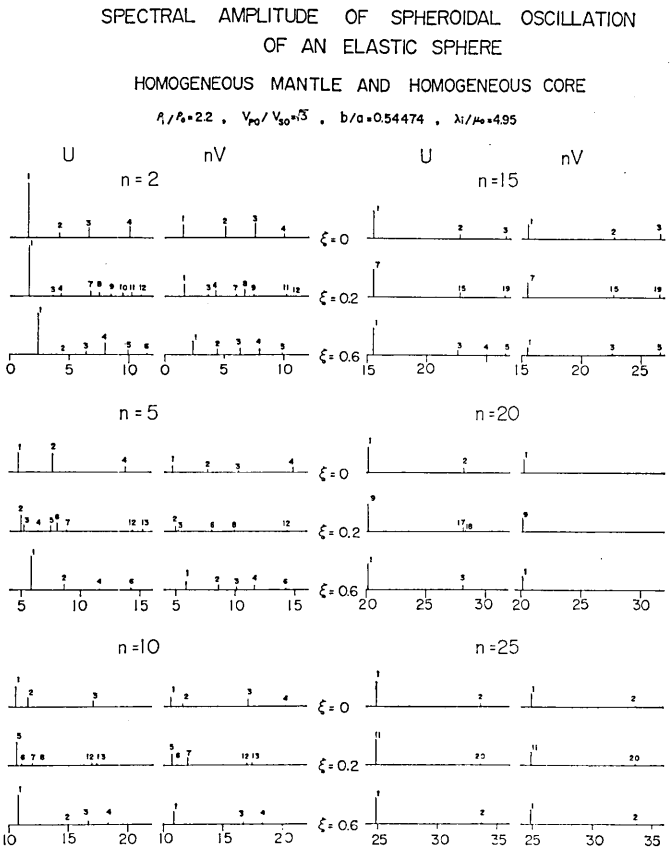

Fig. 3. Spectral amplitude of various modes for the spheroidal oscillation of an elastic sphere consisting of a homogeneous mantle and a homogeneous core as a function of the non-dimensional frequency η. Numbers beside spectral lines indicate the radial mode number i. The missing numbers mean that the corresponding mode has negligibly small spectral amplitude.

displacement in the core. These features are well developed in Figure 2-a, especially for the cases $n=5$, 10 and 15.

It is remarkable, however, that these general features suddenly disappear when the non-dimensional frequency of a mode becomes very close to that of the liquid core, as is shown by the case $n=15$ and $i=7$ in Figure 2-a. In this case the radial distribution resembles that of the liquid core and shows no oscillatory amplitude in the core.

5. Soft Core Spectrum Splitting

The spectral amplitudes of radial and colatitudinal displacements were computed for the three cases $\xi(=V_{Si}/V_{So})=0.0$ (liquid core), 0.2 (soft core) and 0.6 using the formula (2.7) and are presented in Figure 3. When the core is soft, (see the case $\xi=0.2$), there are many spectral lines corresponding to many branches in Figure 1, but not all of them show appreciable amplitude. The number beside the vertical line means the radial mode number i. The missing numbers indicate that the corresponding spectral amplitude is negligibly small.

From the Figure 3, the following can be observed: (1) The case of the liquid core displays widely separated spectral lines, (2) When the core is a soft solid, spectral lines of modes, which have nearly equal frequency to that of the liquid core model, show predominant amplitude, (3) Two adjacent spectral lines corresponding to a certain spectral line of a liquid core sometimes display considerable amplitude, which is a type of spectrum splitting phenomenon (e.g. $\xi=0.2$; $n=10$, $i=12$, 13; $n=20$, $i=17$, 18), (4) The spectral amplitude for the cases $\xi=0.0$, 0.2 and 0.6 shows nearly equal features when the colatitudinal order number n is large or the period is short. This indicates that the short period motion does not penetrate deeply into the earth, showing that the physical property of the core scarecely affects the short period oscillation of the sphere.

6. Transfer from a Soft Solid Core to a Perfect Fluid Core

As is explained in the preceding sections, the free spheroidal oscillation displays the following features when the core is a soft solid:

(a): There appear many more higher radial mode branches as the rigidity of the core decreases;

(b): The radial distribution of displacement in the core shows

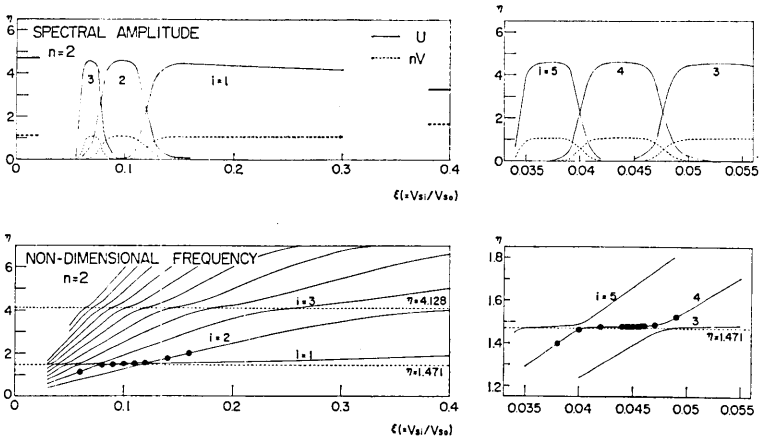
SPECTRAL AMPLITUDE
n=2
U
nV
i=1
i=5
4
3
2
NON-DIMENSIONAL FREQUENCY
n=2
i=3
i=2
i=1
η=4.128
η=1.471
ξ(=Vsi/Vso)

Fig. 4-a

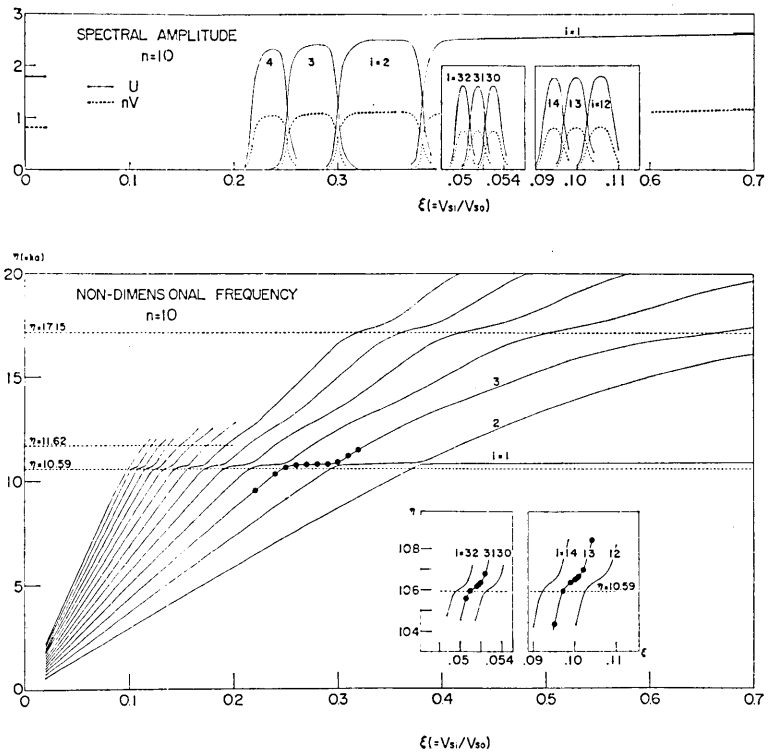
SPECTRAL AMPLITUDE
n=10
U
nV
i=1
i=2
4
3
i=32
i=30
i=14
i=13
i=12
ξ(=Vsi/Vso)
NON-DIMENSIONAL FREQUENCY
n=10
η=17.15
η=11.62
η=10.59
3
2
i=1
ξ(=Vsi/Vso)

Fig. 4-b

oscillatory features and has large amplitude compared with that in the mantle;

(c): The colatitudinal displacements in the mantle and in the core are continuously connected at the core boundary.

On the other hand, the spheroidal oscillation of an elastic sphere with a homogeneous mantle and a liquid core shows that

(a′): Except for a transition branch corresponding to the Stoneley wave along the core-mantle boundary, there appear no special radial higher modes;

(b′): As was shown in a former paper[5], the displacement is larger in the mantle than in the core, where the motion diminishes exponentially as the depth increases;

(c′): The colatitudinal displacement has a discontinuity at the core boundary.

The corresponding items reveal radically different features. Thus, the question arises: "How can these mutually contradictory characteristics be related when the core rigidity tends to zero?"

In order to clarify this transitional feature, the non-dimensional frequency and the displacement distribution of the free spheroidal oscillation are calculated as functions of ξ, the ratio of S wave velocity in the core and mantle. The results are prepared in Figures 4 and 5. The frequency curve in Figure 4 shows the transition phenomenon near the frequency of a liquid core. The upper figure shows the spectral amplitude of the radial and colatitudinal displacements on the surface of a sphere. Radial distributions of displacements for modes corresponding to the dots in the lower figure of Figure 4 are given in Figure 5.

From these Figures the following conclusions are deduced.

1) The transition phenomenon from one radial mode to the next is seen near the non-dimensional frequency of the liquid core model.

2) Only the modes on the transition segments show large spectral amplitude. Consequently, the other parts of the frequency curve can

Fig. 4. Non-dimensional frequency and spectral amplitude as functions of $\xi(=V_{si}/V_{so})$. Horizontal dotted lines in the lower figure indicate the non-dimensional frequency when the core is liquid. Dots show modes whose radial distribution of displacement is given in Figure 5. A part of the figure is given in an enclosure in magnified scale. In the upper figure, representing the spectral amplitude, solid and dotted lines refer to the radial and colatitudinal components respectively. Thick solid and dotted lines on the left and right of the upper figure are the limiting values of spectral amplitude when ξ tends to 0 and 1 respectively. These figures show that the spectral amplitudes of modes on transition segments parallel to the abscissa are predominant.

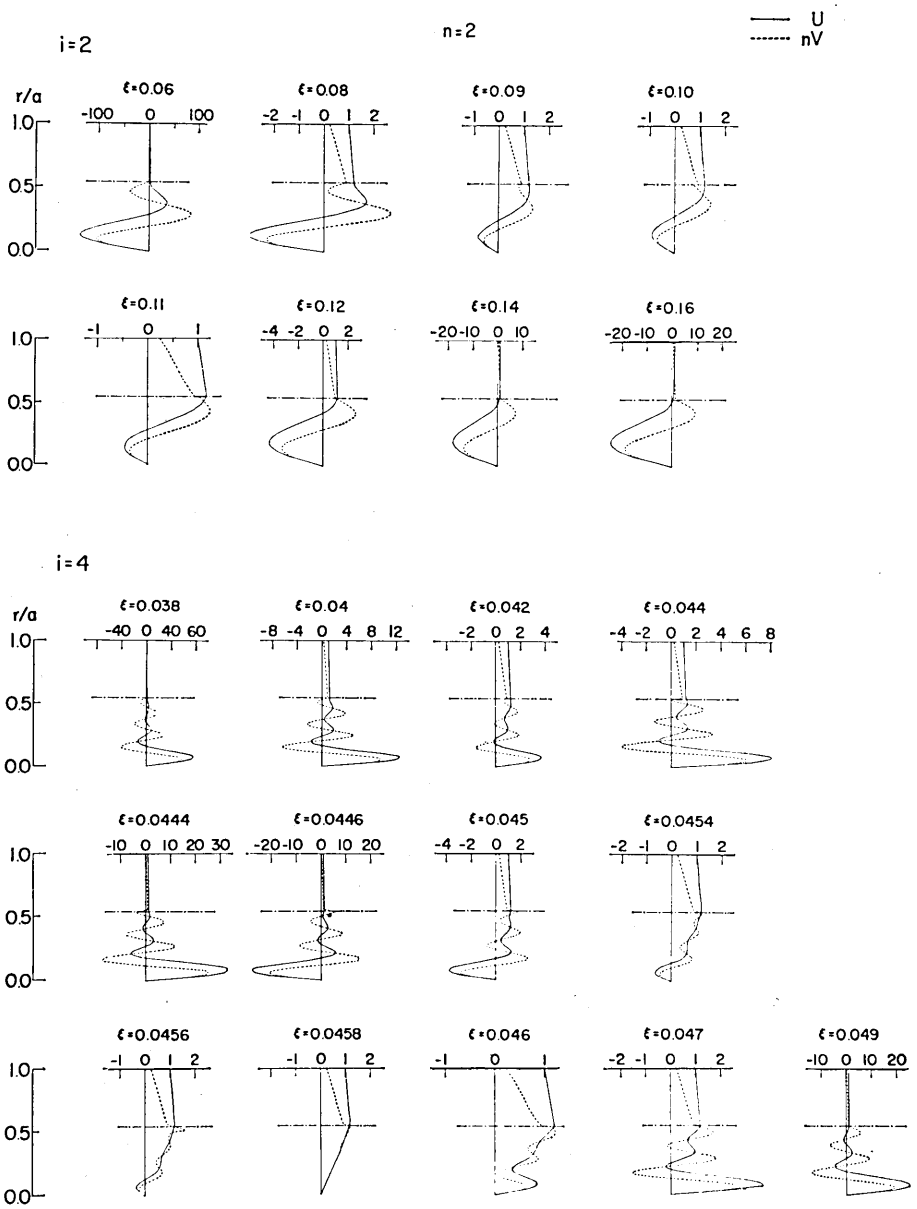
RADIAL DISTRIBUTION OF AMPLITUDE
SPHEROIDAL OSCILLATION
HOMOGENEOUS MANTLE AND HOMOGENEOUS CORE
n=2
U
nV
i=2
r/a
ε=0.06
ε=0.08
ε=0.09
ε=0.10
ε=0.11
ε=0.12
ε=0.14
ε=0.16
i=4
ε=0.038
ε=0.04
ε=0.042
ε=0.044
ε=0.0444
ε=0.0446
ε=0.045
ε=0.0454
ε=0.0456
ε=0.0458
ε=0.046
ε=0.047
ε=0.049

Fig. 5-a

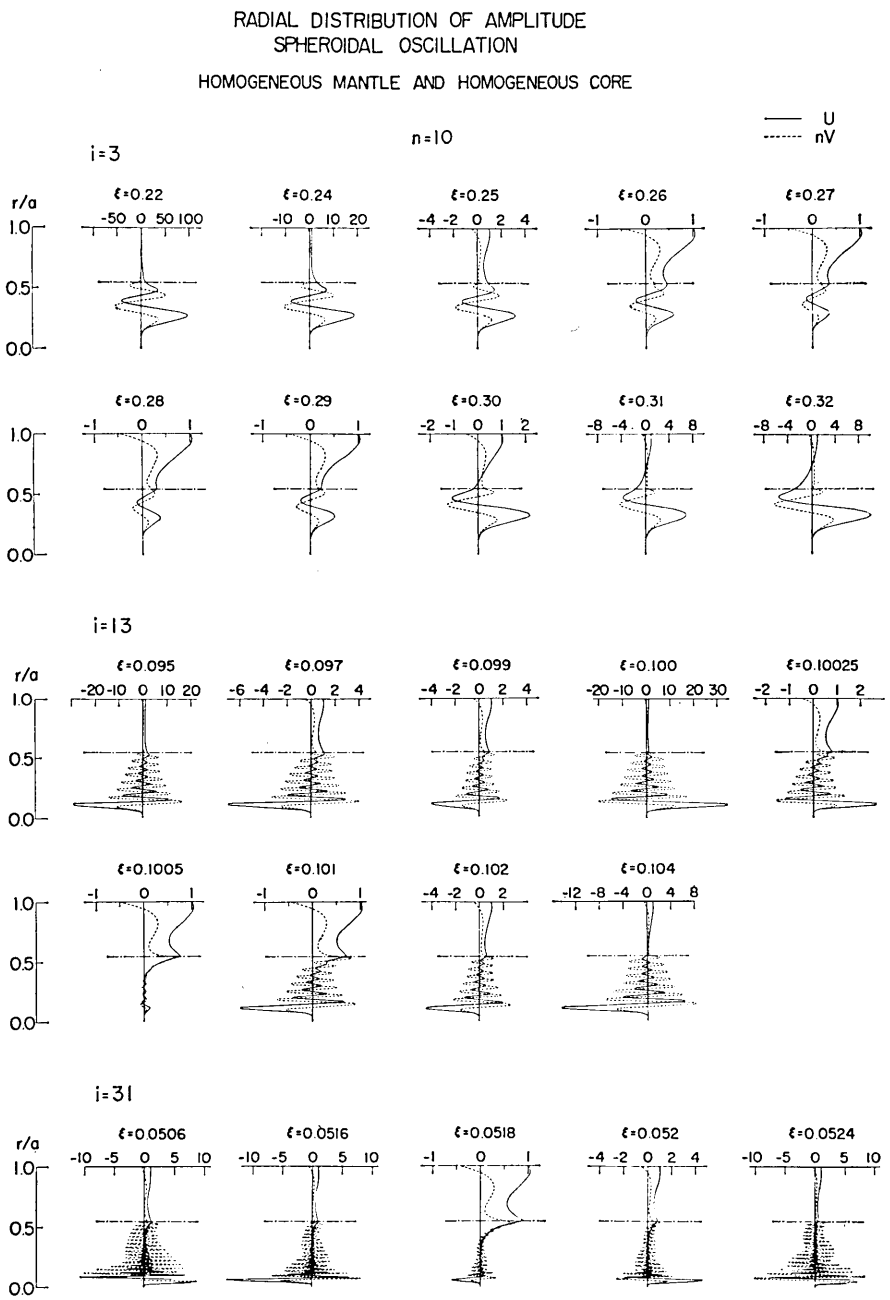

Fig. 5-b

Fig. 5. Radial distribution of displacements for the modes shown by dots in Figure 4. The solid and dotted lines refer to the radial and colatitudinal components respectively. The value of the radial displacement on the surface is taken to be one. Chain line denotes the boundary between the core and mantle.

be neglected as far as the contribution to the surface displacement is concerned.

3) There is a point on each branch which displays a radial distribution of displacement quite similar to that for the case of a liquid core. The rigidity of the core corresponding to this mode will be called the "characteristic core rigidity".

4) The radial distribution of displacement is sharply affected by the value of $\xi(=V_{Si}/V_{So})$. Consequently, a small change in ξ results in a big discrepancy in the pattern of the displacement distribution.

7. Characteristic Core Rigidity

It is seen in Figure 5 that, when the radial distribution of displacement for the case of a soft core resembles that of a liquid core, the oscillatory displacement distribution in the core disappears. Since the oscillatory distribution in the core stems from the $S2$ wave, it is expected that there exist special values of the core rigidity which make the $S2$ waves in the core vanish. This circumstance is proved numerically by the Table 1.

The values in Gothic letter were calculated by numerical interpolation. Therefore, "the characteristic core rigidity" is defined here as the value of core rigidity which makes the $S2$ wave in the core vanish. This means that the characteristic value of the core rigidity satisfies the simultaneous equations

Table 1.

n	$\xi(=V_{Si}/V_{So})$	$\gamma(=ka/V_{So})$	C
2	0.0452	1.4795	0.9364
	0.0454	1.4799	0.3731
	0.0456	1.4802	0.2335
	0.04578	**1.4806**	**0.000**
	0.0458	1.4806	−0.00387
	0.0460	1.4811	−0.3132
10	0.0516	10.6137	0.3572
	0.0518	10.6210	0.0151
	0.05182	**10.6220**	**0.000**
	0.0520	10.6326	−0.1171
	0.0522	10.6514	−0.2750

C: coefficient of $S2$ waves in the core.

$$\overline{\Delta}(6;6)=0, \quad \text{Coefficient of } S2 \text{ wave,} \tag{7.1}$$

$$\text{and} \qquad \Delta=0, \quad \text{Characteristic equation.} \tag{7.2}$$

In Figure 6, the relation between the non-dimensional frequencies satisfying (7.1) and (7.2) are schematically shown. The characteristic value is not found for large values of ξ. The spectral amplitude becomes a maximum near this characteristic value. As ξ decreases, the maximum becomes sharper and the characteristic value appears at shorter intervals. The non-dimensional frequency corresponding to this maximum is, for the case treated, usually larger than that for the liquid core (see Figures 4 and 6). Therefore, when the rigidity of the core is small, namely $\xi \leqq 0.1$, the observed frequency is nearly equal to, but slightly larger than, that of the liquid core. This is the case of "over-frequency" by the terminology in a former paper[3]. The case "under-frequency" is

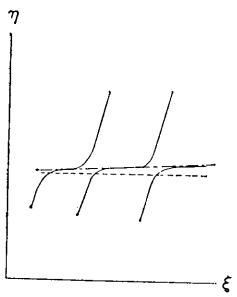

Fig. 6. Schematic figure showing the relation between the non-dimensional frequencies satisfying equation (7.1) (chain line) and (7.2) (solid line). Cross points of these curves give the solution for which the displacement distribution is similar to the case of liquid core. Dotted line refers to the frequency for a perfect liquid core. The ordinate and abscissa are the non-dimensional frequency η and $\xi(=V_{Si}/V_{So})$ respectively.

difficult to detect for the case considered in this and in the preceding sections. In the torsional oscillation, as is explained in the above-mentioned paper, the cases of over-, double- and under-frequencies are readily observed.

8. Concluding Remarks

An elastic sphere consisting of a homogeneous mantle and a homogeneous core is assumed in this paper. The effect of small rigidity of the core on the frequency, the spectral amplitude and the displacement distribution of the spheroidal free oscillation are studied numerically. The following features are noted:

(1) The phenomenon of soft core spectrum splitting will appear for the spheroidal oscillations.

(2) The observed period will differ little from the period for the liquid core.

(3) For special values of core rigidity, which will be called "the characteristic core rigidity", the displacement distribution shows features quite similar to that of the perfect liquid core.

(4) When we observe the earth's free oscillation the observed frequency is likely to be larger than the liquid core frequency. (See Figure 4-a below.) However, the relation between the observed and the liquid core frequency may be reversed for a mode which has a larger frequency for the case $\xi=0$ (liquid core) than for the case $\xi=1$.

(5) The transitional features from a soft solid core to a perfect liquid one are found to be continuous with regard to the period, the spectral amplitude and the displacement distribution.

Although a simple model is adopted in this study, the same principles (1)～(5) above will also hold for an actual earth model with a small core rigidity.

The numerical calculation was carried out on an IBM 7090 through the project UNICON, to which our sincere thanks are due.

48. 等質等方のマントルと核から成る弾性球のスフェロイド型振動のソフト・コア・スペクトル・スプリッティングとこれに関連した問題

地震研究所 宇佐美龍夫 小竹美子 佐藤泰夫

1. 柔らかい核（核の剛性率が零でない小さい値をとるとき）をもつ弾性球のスフェロイド型振動をしらべた.

2. 柔らかい核の影響を明らかにするため，簡単なモデルを採用した．球の半径 $a=6370$ km，核の半径 $b=3470$ km，$b/a=0.544741$，核とマントルの密度の比 $\rho_i/\rho_0=2.2$，マントルでは $\lambda_0=\mu_0$，また $\lambda_i/\mu_0=4.95$ とした．このモデルは核の剛性率が零になると，我々が理論地震記象の研究に使ったモデル[5]と一致する．λ_i は一定に保ち，重力の効果は考慮しなかった.

3. 柔らかい核によるスペクトル分裂をしらべた.

a) $\xi(=Vs_i/Vs_0)=0.2$ と 0.6 の場合についてスフェロイド型振動の固有周波数とそれに対する半径方向の振巾分布を計算した．$\xi=0.2$ の時には沢山の高調波が生じ振巾は核の中で大きくなり，核内での節球面の数は高調波の次数 i とともに増加する．しかし周波数が液体核の周波数に近い値をとるときは（例えば $n=15$, $i=7$, $\xi=0.2$）その振巾分布は流体核の場合に似る.

b) 各モードの表面振巾のスペクトルを計算した．核が柔らかい時には，流体核の周波数に近い周波数をもつモードのスペクトルが卓越する．流体核のスペクトルに対応して，二つの相隣るスペクトルが，かなりの振巾をもつ（ソフト・コア・スペクトル・スプリッティング）ことがある．また n が大きい（周期が小さい）と核の影響は少なくなり ξ に拘らずスペクトルは同じような様子を示す.

4. 柔らかい核の場合には，i) 核の剛性率が小さくなると流体核の場合の高調波分枝に比して，沢山の高調波の分枝が表われる．ii) 核内の変位はマントル内よりはるかに大きく，多数の節球面をもつ．iii) 緯度方向の変位は核の境界で連続である.

一方流体核の場合には，1′) 変位はマントル内で大きく，核の中では深さとともに指数函数的に減る．2′) 緯度方向の変位は核の境界で不連続となる.

核の剛性率が小さくなった極限において，この一見矛盾する性質がどのようにつながるかを調べた．$n=2$ と 10 の場合に $\xi(=Vs_i/Vs_0)$ の函数として固有振動の周波数とスペクトル振巾及び半径方向の振巾分布を計算した．その結果次の事が分かった.

1) 流体核の周波数の近くで，一つの高調波分枝から次の高調波に遷移する．2) この遷移分枝上のモードのスペクトル振巾だけが卓越する．3) 各高調波分枝上に一点があり，そこのモードの振巾分布は流体核の場合に似ている．この点の核の剛性率を“特性剛性率”と呼ぶことにする．4) 振巾分布は ξ の値によって著しく影響される.

5. “特性剛性率”を核内の $SV(S2)$ 波が零になるような剛性率と定義する．この特性値は ξ が大きいと存在しない．ξ が小さいと高調波の各分枝に1つずつある．この特性値の近くでスペクトル振巾は最大となる.

その周波数は常に流体核の場合より大きい．つまり，所謂[3]「オーバー・フリクエンシイ」の場合だけが観測されやすい．しかし，$\xi=1$ の時より $\xi=0$ の時の方が周波数が大きくなるようなモードでは，「アンダー・フリクエンシイ」の場合だけが観測されると考えられる.

6. 簡単なモデルを使って求められた上記の結果は実際の地球モデルの時にも通用すると考えられる.